

**WAVELET BASED CNN FOR DIAGNOSIS OF LUNG  
DISEASES USING CHEST X-RAYS**

**A Project Report**

*Submitted by*

**Ms. JUMANA R**

**REG NO : TKM21MEAI06**

*In partial fulfillment for the award of the degree of*

**MASTER OF TECHNOLOGY**

**IN**

**Mechanical Engineering (Artificial Intelligence)**

**Under the guidance of  
Prof. CHINNU JACOB**



**JULY 2023**

## DECLARATION

I undersigned hereby declare that the project report “WAVELET BASED CNN FOR DIAGNOSIS OF LUNG DISEASES USING CHEST X-RAYS”, submitted for partial fulfillment of the requirements for the award of degree of Master of Technology of the APJ Abdul Kalam Technological University, Kerala is a bonafide work done by me under supervision of Prof. Chinnu Jacob. This submission represents my ideas in my own words and where ideas or words of others have been included, I have adequately and accurately cited and referenced the original sources. I also declare that I have adhered to ethics of academic honesty and integrity and have not misrepresented or fabricated any data or idea or fact or source in my submission. I understand that any violation of the above will be a cause for disciplinary action by the institute and/or the University and can also evoke penal action from the sources which have thus not been properly cited or from whom proper permission has not been obtained. This report has not been previously formed the basis for the award of any degree, diploma or similar title of any other University.

Place: Kollam

Date:

JUMANA R

Thangal Kunju Musaliar College of Engineering  
Centre for Artificial Intelligence



C E R T I F I C A T E

This is to certify that, this report titled ***WAVELET BASED CNN FOR DIAGNOSIS OF LUNG DISEASES USING CHEST X-RAYS*** is a bonafide record of the **project** presented by **JUMANA R (TKM20MEAI06)**, under our guidance and supervision, in partial fulfillment of the requirements for the award of the degree, **M.Tech in Mechanical Engineering (Artificial Intelligence)** in **APJ Abdul Kalam Technological University** .

Project Coordinator and Guide

Prof. Chinnu Jacob  
Assistant Professor  
Centre for Artificial Intelligence

Internal Examiner

Head of the Department

Dr. Imthias Ahamed T P  
Professor  
Centre for Artificial Intelligence

External Examiner

## ACKNOWLEDGEMENT

A successful project is a fruitful culmination of efforts by many people, some directly involved and some others indirectly, by providing support and encouragement. Firstly I would like to thank the almighty for giving me the wisdom and grace for making my project a memorable one. I thank him for steering me to the shore of fulfillment under his protective wings.

I express my sincere gratitude to **Dr. T A Shahul Hameed** , Principal of T.K.M College of Engineering for giving me an opportunity to present my project. I would like to thank **Dr. Imthias Ahamed T P**, Professor and Head of the Department, Centre for Artificial Intelligence, TKM College of Engineering, Kollam, for his constant support and encouragement throughout the project work.

With a profound sense of gratitude, I would like to express my heartfelt thanks to my guide and mini Project co-ordinator, **Prof. Chinnu Jacob**, Assistant Professor, Centre for Artificial Intelligence(AI), TKM College of Engineering, Kollam, for her guidance, cooperation and immense encouragement. I also extend my thanks to the entire faculty and staff members of the Centre for AI, TKMCE, who have encouraged me throughout this work.

I also express my thanks to my loving parents and friends, for their support and encouragement in the successful completion of this work.

JUMANA R

## Abstract

Lung diseases are widespread worldwide, including conditions such as lung nodules, pneumonia, asthma, tuberculosis, fibrosis, etc. It is crucial to diagnose lung disease promptly. In this study, wavelet-based Convolutional Neural Networks have been employed to detect and differentiate various types of lung diseases through analyzing chest X-ray images. Existing CNN architectures have been used previously to classify healthy and affected condition chest X-rays. However, these networks process the image in a single resolution and may lose potential features present in other resolutions of the input image. Over this normal CNN, Wavelets are utilized to decompose the image into different spatial resolutions based on high pass and low pass frequency components and extract valuable features from the affected portion of lung X-ray images efficiently. A CNN model of wavelet is employed to find relevant features from the X-ray images, and SVM classifier is incorporated to classify different lung diseases from the extracted features. The proposed framework is tested on three publicly available datasets and the method achieved an average accuracy of 100% using the first dataset (NIH Chest X-ray), 100% accuracy on the second dataset (LUNG DISEASE), and 96% accuracy on the third dataset (JSRT). Overall, the proposed approach outperformed existing works and demonstrated its effectiveness in identifying multiple lung conditions, including nodules, COVID-19, and other ailments, making it a versatile tool.

# Contents

- 1 Introduction** **1**
  - 1.1 Objective(s) . . . . . 2
  - 1.2 Organization of the report . . . . . 3
  
- 2 Literature Survey** **4**
  
- 3 Methodology** **7**
  - 3.1 Wavelet Convolutional Neural Networks . . . . . 7
  - 3.2 Enhancing Image Analysis with Wavelet CNN: Advantages over Traditional CNN . . . . . 8
  - 3.3 Proposed Method . . . . . 8
    - 3.3.1 Preprocessing(Data Sandardization and Normalization) . . . . . 9
    - 3.3.2 Feature extraction using Wavelet CNN . . . . . 9
  - 3.4 Proposed Architecture details . . . . . 11
  - 3.5 SVM classifier . . . . . 13
  - 3.6 Performance Evaluation . . . . . 14
  
- 4 Experimental Analysis and Results** **15**
  - 4.1 Experimental Setup . . . . . 15
  - 4.2 Datasets . . . . . 15
  - 4.3 Confusion matrix . . . . . 17
  - 4.4 ROC - AUC . . . . . 19
  - 4.5 Comparison with Existing Works . . . . . 20
  
- 5 Conclusion** **23**
  
- References** **24**

# List of Figures

3.1	General Block diagram of proposed method . . . . .	9
3.2	Layers Design of Proposed System . . . . .	11
4.1	Chest xray samples from dataset . . . . .	16
4.2	Confusion matrix of proposed model using NIH dataset . . . . .	17
4.3	Confusion matrix using Lung disease dataset . . . . .	19
4.4	Confusion matrix using JSRT dataset. . . . .	20
4.5	ROC-AUC curve of proposed model using JSRT dataset . . . . .	22

# List of Tables

3.1	Architecture details of proposed method . . . . .	12
4.1	Performance metrics of proposed model using NIH dataset . . . . .	18
4.2	Performance metrics of proposed model using Lung disease dataset . . . . .	18
4.3	Performance metrics of proposed model using JSRT dataset . . . . .	20
4.4	Comparison between different classifiers using NIH dataset . . . . .	21
4.5	Comparison between different classifiers using Lung disease dataset . . . . .	21
4.6	Comparison between different classifiers using JSRT dataset . . . . .	22
4.7	Comparison with Existing Works . . . . .	22

# Chapter 1

## Introduction

The adverse effects of changing climatic conditions on human health are getting more and worse today. Because of the rapid increase in diseases, there has been a significant increase in the number of people who passed away. The most serious illnesses that have caused the most fatalities in recent years are lung diseases. According to the World Health Organization (WHO), more than 60 million people worldwide suffer from the negative impacts of chronic obstructive pulmonary disease (COPD), and about 3 million people pass away from it each year, making it the third leading cause of fatalities in the period 2019–2020. It is estimated that 10 million people worldwide have various lung diseases, and that 1.6 million die from them each year, making it the infection with the highest mortality rate. Lung cancer is the most lethal illness, claiming the lives of around 1.7 million people annually. Asthma is the most well-known chronic infantile disease, affecting 14% of children worldwide, and it is still on the rise, affecting more than 330 million people worldwide[1][2].

Developing and low-income countries are particularly vulnerable to the risks associated with lung diseases due to the combination of poverty and air pollution. These nations often lack access to clean fuels and efficient cooking technologies, leading to high levels of household air pollution. The WHO estimates that each year, approximately 4 million premature deaths occur as a direct result of diseases related to household air pollution. These diseases include asthma, pneumonia, chronic obstructive pulmonary disease (COPD), and lung cancer. Reducing air pollution and carbon emissions is crucial in mitigating the impact of lung diseases in these regions. This requires implementing effective policies and strategies to promote clean energy sources, improve indoor air quality, and minimize environmental pollutants. Investing in renewable energy, promoting sustainable transportation, and adopting cleaner industrial practices are essential steps to reduce the burden of air pollution.

In addition to tackling air pollution, early detection and diagnosis of lung diseases play a vital role in minimizing their adverse effects. Implementing efficient diagnostic systems in healthcare settings can significantly aid in the early identification and management of lung disorders. This includes the use of advanced imaging technologies, such as X-ray, computed tomography (CT) scans, pulmonary function tests, and biomarker analysis.

Since late December 2019, the world has been grappling with the emergence of the novel coronavirus disease 2019 (COVID-19). This infectious disease primarily affects the respira-

tory system, causing severe lung damage and leading to breathing difficulties. COVID-19 can result in pneumonia, a type of lung disease, either directly through the viral infection or as a secondary infection due to a weakened immune system. It is crucial to continue researching and implementing effective strategies to prevent, diagnose, and treat COVID-19 and its associated lung complications[3].

Addressing the risks of lung diseases requires a comprehensive approach that encompasses reducing air pollution, promoting clean energy sources, enhancing diagnostic capabilities, and effectively managing infectious diseases. International collaboration, public awareness campaigns, and policy interventions are key to ensuring a healthier future for individuals living in developing and low-income countries, where the burden of lung diseases is disproportionately high.

Chest X-rays are commonly used by radiologists as a primary diagnostic tool for detecting and classifying various lung illnesses. With over 2 million procedures conducted each year, chest X-rays are the most widely employed diagnostic imaging technique globally. They have proven to be effective in identifying a wide range of lung conditions, such as infections, tumors, and structural abnormalities. The accessibility, cost-effectiveness, and ability to provide immediate results make chest X-rays a valuable tool in the diagnostic process.

The early detection of lung disorders has become more important than any time in the recent past. Deep learning (DL) and artificial intelligence (AI) can play a crucial role in this. The DL framework based on chest X-rays may be valuable for recognising and assessing lung diseases, according to researchers from all around the world[4],[5],[6],[7]. The main field of research for improving computer-aided diagnosis has been intelligent computational algorithms for categorising and identifying diseases. Medical professionals may misinterpret real infections as a result of similarities between the symptoms of numerous diseases. In countries with tropical climates, where communicable diseases often exhibit similarly upon detection, such complications are quite frequent, and the ensuing delay in disease diagnosis and treatment may result in life-threatening consequences for patients of all ages.

This study aims to provide guidance for using the DL framework to diagnose lung-related illnesses. The framework presented here can help in correctly classifying the various lung conditions, which can lead to the early detection and treatment of deadly diseases, so preventing further effects.

## 1.1 Objective(s)

The objective of this work is :

- To develop a wavelet-based Convolutional Neural Network for detecting and differentiating various types of lung diseases through analyzing chest X-ray images.
- To employ wavelet decomposition to extract valuable features from the diseased portion of lung X-ray images efficiently.

- To incorporate different classifiers to classify the type of lung diseases such as lung nodules, pneumonia, asthma, tuberculosis, fibrosis, etc. from the extracted features.
- To test the proposed framework on publicly available datasets and evaluate its performance in terms of accuracy.

### 1.2 Organization of the report

The paper can be organized as follows: Section 2 describes some related works on lung X-ray image classification or lung nodule detection and classification. The problem statement and methodology of this work are presented in Section 3. A detailed analysis of the implemented dataset, results and associated discussion are presented in Section 4. while Section 5 concludes the paper.

## Chapter 2

# Literature Survey

Many research projects have been undertaken to illustrate the steps and techniques for identifying various lung diseases using chest x-ray images. Below are a few important studies that have been done in this field.

Vieira, P., et al. [8] proposed Detection of pulmonary diseases using deep features in X-ray images. Deep learning techniques have been applied to detect COVID-19 pneumonia in X-ray images, facilitating fast and accurate diagnosis. In this study, seven deep learning architectures, along with data augmentation and transfer learning techniques, were investigated for detecting various pneumonia types. The results were promising, achieving an accuracy of 99.8% for classifying COVID-19, normal, viral, and bacterial pneumonia.

Ismael, A.M., et al. [9] presented Deep learning approaches for COVID-19 detection based on chest X-ray images. In this study, deep learning techniques, including deep feature extraction, fine-tuning of pretrained convolutional neural networks (CNN), and end-to-end training of a new CNN model, were employed to classify COVID-19 and normal chest X-ray images. Support Vector Machines (SVM) with various kernel functions were employed for classification. The highest accuracy score of 94.7% was achieved by the combination of deep features extracted from the ResNet50 model and SVM classifier with the Linear kernel function.

Shah, P.M. et al. [10] presented Deep GRU-CNN model for COVID-19 detection from chest X-rays data. In this paper, the researchers propose a hybrid deep learning model that combines a convolutional neural network (CNN) and a gated recurrent unit (GRU) to detect COVID-19 from chest X-ray images. The CNN is utilized for feature extraction, while the GRU acts as a classifier. The model is trained on a dataset of 424 chest X-ray images, categorized into three classes: COVID-19, pneumonia, and normal. It achieves precision, recall, and f1-score values of 0.96, 0.96, and 0.95, respectively.

Mehrrotraa, R. et al. [11] developed Ensembling of efficient deep convolutional networks and machine learning algorithms for resource effective detection of tuberculosis using thoracic (chest) radiography. In this study, they proposed an ensemble approach that combines efficient deep convolutional networks and machine learning algorithms to enable resource-effective detection of TB. Three highly efficient deep convolutional networks and machine

## WAVELET BASED CNN FOR DIAGNOSIS OF LUNG DISEASES USING CHEST X-RAYS

---

learning algorithms are utilized for the identification of TB. The proposed model achieved an accuracy rates of 87.90% in identifying TB-infected images compared to normal and COVID-19-infected images, respectively.

Bharati, S., et al. [12] developed Hybrid deep learning for detecting lung diseases from X-ray images. The basic CNN model often struggles with images that are rotated, tilted, or have abnormal orientations. To overcome this limitation, a hybrid deep learning framework called visual geometry group based neural networks(VGG) Data STN with CNN (VDSNet) is proposed in this study. The VDSNet combines VGG, data augmentation, and spatial transformer network (STN) with CNN to enhance performance. For the full dataset, VDSNet achieves a validation accuracy of 73%.

Li, X., et al. [13] developed Multi-resolution convolutional networks for chest X-ray radiograph based lung nodule detection. This paper introduces a deep learning-based method for lung nodule detection, utilizing patch-based multi-resolution convolutional networks and four fusion methods for classification. In experiments using the Japanese Society of Radiological Technology (JSRT) database, over 99% of lung nodules were detected with a false positives per image (FPs/image) rate of 0.2. The proposed method achieved high FAUC and R-CPM values of 0.982 and 0.987, respectively, indicating its potential for clinical applications.

Makris et al. [14] presented COVID-19 detection from chest X-Ray images using Deep Learning and Convolutional Neural Networks. The study aimed to utilize technology for assisting in COVID-19 diagnosis by evaluating pre-trained CNNs for detecting infected patients from chest X-ray images. A mixed dataset containing COVID-19, bacterial pneumonia, and healthy individuals' X-ray images was created. Transfer learning was employed to overcome the limited sample size. The experimental results demonstrated up to 95% accuracy, with VGG16 and VGG19 achieving the best performance.

de Moura, J. et al. [15] proposed Fully automatic deep convolutional approaches for the analysis of COVID-19 using chest X-ray images. The paper proposes four fully automatic approaches for the classification of chest X-ray images into three categories: Covid-19, pneumonia, and healthy cases. The study addresses the challenge of differentiating between Covid-19 and pneumonia during the initial stages of the diseases, considering different pathological scenarios. The obtained accuracy values are 0.9706, 0.9839, 0.9744, and 0.9744, respectively, for the classification of chest X-ray images into the categories of Covid-19, pneumonia, and healthy cases.

Ayan, E. et al. [16] presented Diagnosis of pediatric pneumonia with ensemble of deep convolutional neural networks in chest X-ray images. The study proposed a CNN ensemble method for the automatic diagnosis of pneumonia in chest X-ray images, focusing on cases in children. Seven different CNN models, including VGG-16, VGG-19, ResNet-50, Inception-V3, Xception, MobileNet, and SqueezeNet, were trained using transfer learning and fine-tuning strategies. The proposed ensemble method achieved a classification accuracy of 90.71 for normal, viral pneumonia, and bacterial pneumonia cases in chest X-ray images.

Li, C., et al. [17] presented False-positive reduction on lung nodules detection in chest radiographs by ensemble of convolutional neural networks. The paper proposes an ensemble of convolutional neural networks (E-CNNs) framework for reducing false positives in the detection of lung nodules in chest radiographs (CXRs). The framework includes the use of unsharp mask technique for nodule enhancement and the construction of three optimized CNNs with different input sizes and depths. The results show that the proposed E-CNNs achieve a sensitivity of 94% and 84% with an average of 5.0 false positives per image and 2.0 false positives per image, respectively. The E-CNNs model demonstrates promising results with a sensitivity of 92% and 5.0 false positives per image in a practical use case.

Hemdan et al. [18] have proposed a novel deep learning algorithm called COVIDX-Net: A Framework of Deep Learning Classifiers to Diagnose COVID-19 in X-Ray Images. This framework utilizes seven deep learning classifiers, including VGG19, DenseNet121, ResNetV2, InceptionV3, InceptionResNetV2, Xception, and MobileNetV2, to automatically identify and confirm COVID-19 in 2-D X-ray images. The VGG19 and DenseNet models demonstrated strong performance in automated COVID-19 classification, achieving f1-scores of 0.89 and 0.91 for normal and COVID-19 cases, respectively. On the other hand, the InceptionV3 model exhibited the poorest classification performance, with f1-scores of 0.67 for normal cases and 0.00 for COVID-19 cases.

Kakde et al. [19] has proposed an Optimal Classification of COVID-19: A Transfer Learning Approach. This paper addresses the challenge of analyzing and diagnosing COVID-19 by focusing on the classification of COVID-19 with normal chest X-ray images using deep learning techniques. The dataset consisted of two classes and was relatively small, making transfer learning necessary. Analysis with two and three fully connected layers was conducted, and results indicated that two fully connected layers with batch normalization achieved better performance in terms of test loss (0.0477) and p-score (0.9643).

Yasar, H., Ceylan, M., et al. [20] have proposed, A new deep learning pipeline to detect Covid-19 on chest X-ray images using local binary pattern, dual tree complex wavelet transform and convolutional neural networks. This study focused on early diagnosis of COVID-19 using X-ray images and employed deep learning techniques, specifically convolutional neural networks (CNN). Two CNN architectures with 23 and 54 layers were developed. Additionally, image processing techniques such as dual tree complex wavelet transform (DT-CWT) and local binary pattern (LBP) were applied to the X-ray images. Four new result generation pipeline algorithms were proposed to improve the study's success. For the first training-test dataset, the accuracy was found to be 0.9843. For the second training-test dataset, the accuracy was 0.9891. Finally, when all the images were combined in the last training-test dataset, the average highest accuracy obtained was 0.9906.

## Chapter 3

# Methodology

### 3.1 Wavelet Convolutional Neural Networks

Images generally consist of areas that are relatively uniform and continuous, interspersed with a few locations that exhibit sharp angles or abrupt contrast transitions. These abrupt change regions contain the most significant information. However, such data cannot be analysed using the Fourier transform, which represents data as a sum of sine waves that are not localized in time or space. Therefore, an alternative approach is needed that can allow us to analyse such data in both the time and frequency domains, enabling the examination of these critical abrupt change regions.

Wavelet CNN is a deep learning architecture that incorporates wavelet transforms into convolutional neural networks (CNNs) to improve the ability of the network to capture and represent signals in both time and frequency domains. By decomposing the input signal into different scales and frequencies, wavelet CNN can efficiently extract features and patterns from complex signals, such as audio and image data. This approach has shown promising results in various applications, including audio classification and image denoising, making it a powerful tool for signal processing and analysis.

Wavelets are a type of wave that have a finite duration and come in various sizes and shapes. They can be analyzed in both time and frequency domains, making wavelet analysis a powerful tool. The wide variety of wavelets available is one of the major advantages of wavelet analysis. The scaling component of the wavelet transform is a key feature that describes the expansion or compression of the signal in the time domain. When a signal is scaled by a factor of 2, the frequency is halved, and when it is scaled by a factor of 0.5, the frequency doubles. As a result, smaller scale factors correspond to high-frequency, contracted wavelets, while larger scale factors correspond to low-frequency, stretched wavelets. Stretched wavelets are useful for describing gradual changes in an image, while shrunk wavelets can highlight rapid changes.

The second important aspect of the wavelet transform is shifting, which refers to the delay or advancement of the signal. Shifting is necessary to align the signal features accurately. The continuous wavelet transform analyzes the signal at intermediate scales, with each octave using wavelets that capture the oscillatory nature of the signal. This type of

analysis is useful for time-frequency analysis and filtering of localized frequency components. For image and signal denoising and compression, the discrete wavelet transform is the most effective method because it reduces coefficient redundancy and occurs at integer multiples. A multilevel wavelet decomposition, also known as the discrete wavelet transform, can be used to denoise an image by dividing the signal into low-pass and high-pass subbands, or approximation and detail levels. After this division, appropriate thresholding methods can be applied to the data, CNN is utilized, with the output being max- or average-pooled after applying nonlinearity. These stages are repeated to form the layers. Although deep CNNs are powerful, they have some drawbacks, such as requiring significant processing resources and large datasets for both training and testing. In addition, selecting minor network parameters can be time-consuming, and the resulting features may be overly complex. To address these issues, we developed a novel CNN architecture that combines wavelet and conventional convolutional layers, specifically designed for processing small datasets in resource-constrained environments. This approach facilitates the use of CNN models in medical settings to aid radiologists and doctor.

### 3.2 Enhancing Image Analysis with Wavelet CNN: Advantages over Traditional CNN

It has been observed that wavelet-based convolutional neural networks (CNNs) can outperform traditional CNNs in certain applications. Wavelet CNNs utilize wavelet transformations as preprocessing steps before the CNN layers, allowing for improved feature extraction and capturing both local and global image information. This approach has shown promising results in various tasks such as image denoising, image classification, and medical image analysis.

Compared to normal CNNs, wavelet CNNs offer several advantages. By incorporating wavelet transforms, they can effectively handle multi-resolution analysis, which is beneficial for tasks that require capturing details at different scales. The wavelet coefficients can provide additional information about the image structure, enabling better discrimination between different patterns. Additionally, wavelet CNNs have demonstrated improved robustness against noise and distortions in the input images.

### 3.3 Proposed Method

Figure 3.1 shows the general block diagram of proposed method. It aims to enhance the analysis of chest X-ray images by leveraging a wavelet CNN model for feature extraction. The dataset utilized for training and evaluation comprises diverse chest X-ray images representing different lung diseases. The methodology consists of three integral stages: preprocessing, feature extraction, and classification. During preprocessing, the input images undergo essential transformations and enhancements to optimize data quality. Moreover, data augmentation techniques are applied to augment the dataset, thereby enhancing model robustness. The preprocessed images are then fed into the wavelet CNN, which utilizes wavelet transforms to extract features from various directions. By employing wavelet transforms within the

## WAVELET BASED CNN FOR DIAGNOSIS OF LUNG DISEASES USING CHEST X-RAYS

CNN architecture, the model effectively captures both fine and coarse details, incorporating crucial spatial and frequency information. Finally, machine learning classifiers utilize the extracted features to classify various lung diseases accurately.

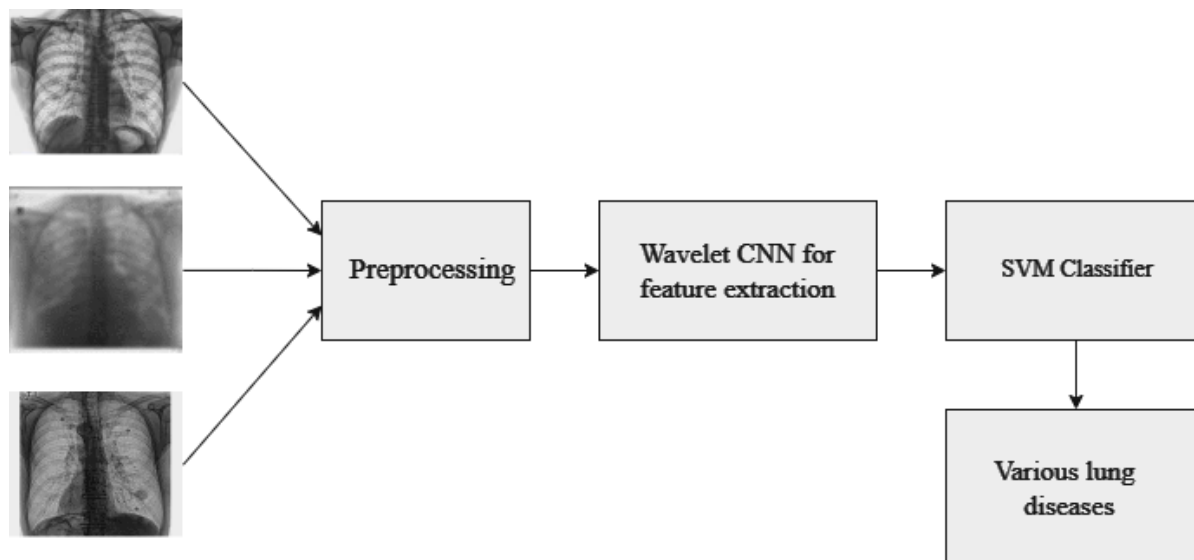


Figure 3.1: General Block diagram of proposed method

### 3.3.1 Preprocessing(Data Sandardization and Normalization)

The preprocessing steps included here are as follows:

- Rescaling: The rescale parameter is set to  $1/255.0$ , which divides each pixel value by  $255.0$  to rescale the image pixel values to the range of  $[0, 1]$ . This step helps to normalize the pixel values and bring them within a manageable range.
- Sample-wise Standard Normalization: The sample-wise standard normalization parameter is set to True, which performs sample-wise standard normalization on the images. This normalization subtracts the mean value of each image and divides it by the standard deviation of that image. It helps to standardize the pixel values across different images and makes the model more robust to variations in pixel intensity.
- Sample-wise Centering: The sample-wise center parameter is set to True, which performs sample-wise centering on the images. This step subtracts the mean value of each image from every pixel in that image. Centering the pixel values around zero helps to remove any bias or offset in the data and can improve model performance.

### 3.3.2 Feature extraction using Wavelet CNN

The wavelet transform is a mathematical technique used for analyzing signals and images. Here, it can be used to decompose an image into different frequency components known

## WAVELET BASED CNN FOR DIAGNOSIS OF LUNG DISEASES USING CHEST X-RAYS

---

as the LL, LH, HL, and HH components. Here's a step-by-step explanation of how these components are calculated:

- Start with the original image, denoted by  $f(x,y)$ , where  $(x,y)$  represents the spatial coordinates.
- Apply a low-pass filter to  $f(x,y)$  to obtain the approximate component, denoted by  $cA$ . This is achieved by convolving  $f(x,y)$  with a low-pass filter, denoted by  $g(x,y)$ . The convolution operation involves multiplying each pixel of the image with the corresponding filter coefficient and summing the results. The resulting values are down-sampled by a factor of 2 in both dimensions.

$$cA(i, j) = \text{sum}(\text{sum}(f(2i - k, 2j - l) * g(k, l))) \quad (1)$$

Here,  $i$  and  $j$  are the row and column indices of the output coefficient array, and  $k$  and  $l$  are the row and column indices of the filter.

- Apply a high-pass filter to  $f(x,y)$  to obtain the detail coefficients in the horizontal direction, denoted by  $cH$ . This is similar to the previous step but involves convolving  $f(x,y)$  with a high-pass filter, denoted by  $h(x,y)$ , that captures the horizontal details.

$$cH(i, j) = \text{sum}(\text{sum}(f(2i - k, 2j - l) * h(k, l))) \quad (2)$$

- Apply a high-pass filter to  $f(x,y)$  to obtain the detail coefficients in the vertical direction, denoted by  $cV$ . This step involves convolving  $f(x,y)$  with a high-pass filter that captures the vertical details.

$$cV(i, j) = \text{sum}(\text{sum}(f(2i - k, 2j - l) * h(k, l))) \quad (3)$$

- Apply a high-pass filter to  $f(x,y)$  to obtain the detail coefficients in the diagonal direction, denoted by  $cD$ . This step involves convolving  $f(x,y)$  with a high-pass filter that captures the diagonal details.

$$cD(i, j) = \text{sum}(\text{sum}(f(2i - k, 2j - l) * h(k, l))) \quad (4)$$

By decomposing the image into these components, the wavelet transform provides a multi-resolution representation of the image, capturing different levels of detail in different frequency bands. The decomposed images obtained from the wavelet transform are passed through the CNN for feature extraction. In this approach, each decomposed image is treated as a separate input channel or a separate input image for the CNN. The CNN is then trained to learn and extract discriminative features from these decomposed images. The convolutional layers of the CNN perform local receptive field operations, capturing and learning relevant patterns and features at different scales and orientations from the decomposed images. During the training process, the CNN learns to automatically detect and extract relevant features from the decomposed images. Utilizing the wavelet transform in conjunction with a CNN, the feature extraction process involves passing the decomposed images obtained from the wavelet transform through the CNN.

### 3.4 Proposed Architecture details

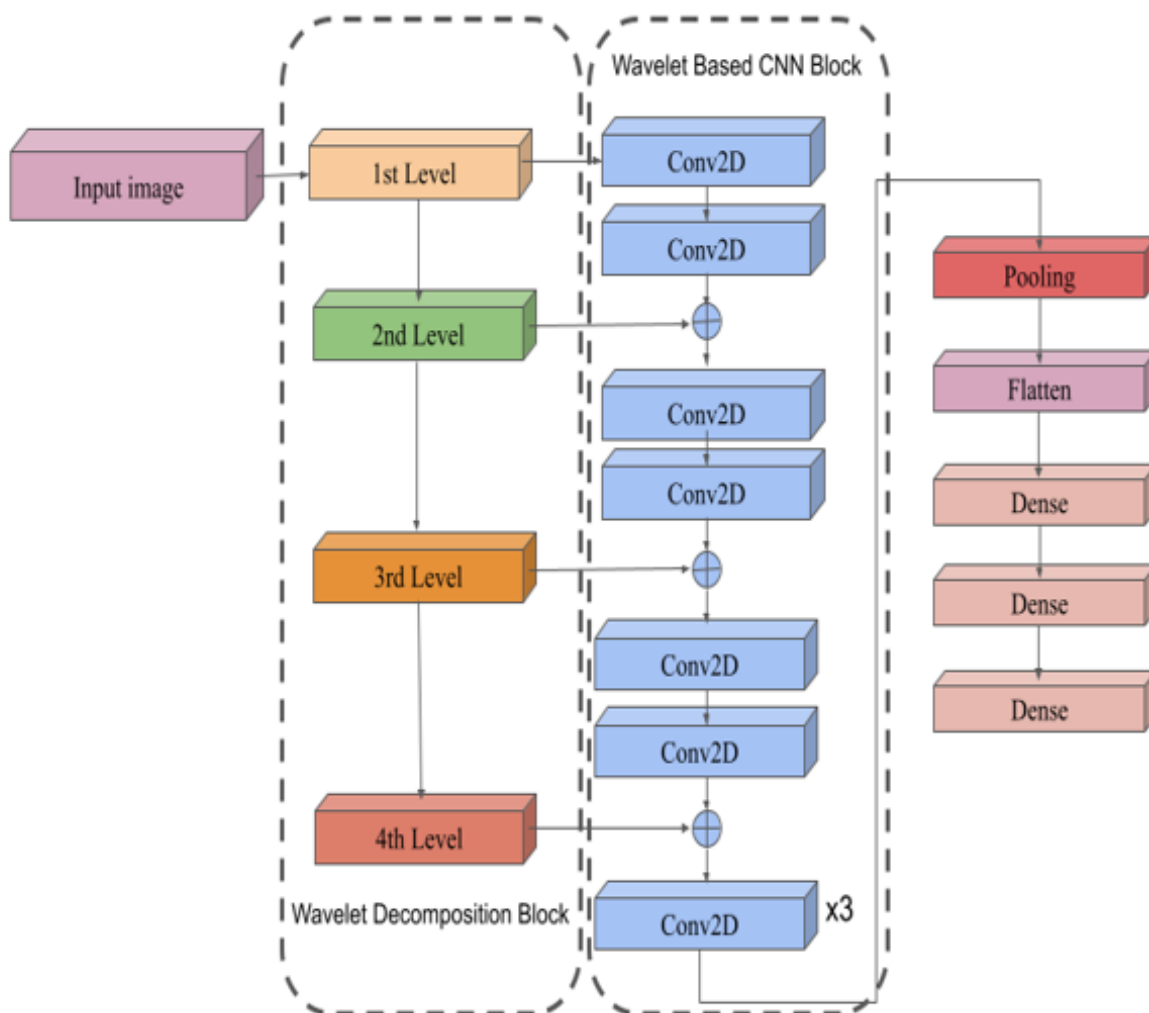


Figure 3.2: Layers Design of Proposed System

The architecture details of the proposed wavelet CNN for diagnosing various lung diseases using chest X-ray images is depicted in Figure 3.2 and Table 3.1. The proposed architecture initiates with a 256x256x3 input representing the chest X-ray image. It employs a wavelet transform technique to decompose the input image into four distinct levels. At each level of decomposition, the input image is processed separately through a series of convolutional layers and batch normalization layers. This allows the model to capture and extract relevant features from the decomposed images at different scales. Starting with the first level, the decomposed images are passed through two convolutional layers, which apply a set of filters to capture spatial patterns. The resulting output from these layers is then concatenated with the second level decomposed wavelet images, combining information from both levels. The concatenated output is further processed through another set of convolutional layers

## WAVELET BASED CNN FOR DIAGNOSIS OF LUNG DISEASES USING CHEST X-RAYS

and batch normalization layers, enabling the model to capture and integrate features from the first and second levels of decomposition. This process helps to refine and enhance the representation of the extracted features.

Similarly, the third level decomposed wavelet images are processed through three convolutional layers. The resulting output is then concatenated with the third level decomposed images, combining the information captured at both levels. This concatenated output undergoes additional convolutional layers to further refine and enrich the extracted features. Finally, the output from the last level of decomposition, along with the processed third level decomposed images, passes through three more convolutional layers. This allows the model to capture high-level features and intricate spatial relationships. The subsequent layers consist of an average pooling layer, which reduces the spatial dimensions, followed by a flattening operation to convert the output into a vector representation. The flattened output is processed through two dense layers and a dense layer with a softmax function at the end. Thus, this architecture performs multi-resolution analysis on the images, processing them in both the spatial and spectral domains, ultimately enhancing the classification performance for various lung disease.

Table 3.1: Architecture details of proposed method

Layer(type)	Output Shape	No. of Filters	Activation	Kernel Size
InputLayer	(256, 256, 3)	-	-	-
conv_1(Conv2D)	(256, 256, 3)	64	relu	(3, 3)
conv_1.2 (Conv2D)	(128, 128, 64)	64	relu	(3, 3)
conv_a (Conv2D)	(128, 128, 64)	64	relu	(3, 3)
conv_2 (Conv2D)	(128, 128, 128)	128	relu	(3, 3)
conv_2.2 (Conv2D)	(64, 64, 128)	128	relu	(3, 3)
conv_b (Conv2D))	( 64, 64, 64)	64	relu	(3, 3)
conv_b.2 (Conv2D)	(64, 64, 128)	128	relu	(3, 3)
conv_3 (Conv2D)	(64, 64, 256)	256	relu	(3, 3)
conv_3.2 (Conv2D)	(32, 32, 256)	256	relu	(3, 3)
conv_c (Conv2D)	(32, 32, 64)	64	relu	(3, 3)
conv_c.2 (Conv2D)	(32, 32, 256)	256	relu	(3, 3)
conv_c.3 (Conv2D)	(32, 32, 256)	256	relu	(3, 3)
conv_4 (Conv2D)	(32, 32, 256)	256	relu	(3, 3)
conv_4.2 (Conv2D)	(16, 16, 256))	256	relu	(3, 3)
conv_5.1 (Conv2D)	(16, 16, 128)	128	relu	(3, 3)
avg_pool_5.1 (AveragePooling2D)	(16, 16, 128)	-	-	(7, 7)
flat_5.1 (Flatten)	(None, 32768)	-	-	-
fc_5 (Dense)	(None, 2048)	67112960	-	-
drop_5 (Dropout)	(None, 2048)	-	-	-
fc_6 (Dense)	(None, 2048)	4196352	-	-
drop_6 (Dropout)	(None, 2048)	-	-	-
fc_7 (Dense)	(None, 15)	30735	softmax	-

## 3.5 SVM classifier

Support Vector Machines (SVM) is a powerful classification technique extensively utilized in the field of medical imaging. SVM is a supervised machine learning algorithm that excels in separating data points into distinct classes by defining an optimal hyperplane. In the context of medical imaging, SVM has been successfully employed for various tasks such as cancer detection, tumor segmentation, and disease classification. Its ability to handle high-dimensional data and capture complex relationships makes it well-suited for analyzing medical images, which often contain intricate patterns and structures. SVM leverages the concept of maximum margin, aiming to find a decision boundary that maximizes the margin between different classes, thereby enhancing generalization and robustness. By effectively mapping input data to a higher-dimensional feature space, SVM can uncover nonlinear relationships and achieve accurate classification results. Its versatility, ability to handle diverse data types, and strong generalization performance make SVM a valuable tool in medical image analysis and contribute to advancements in diagnosis, prognosis, and treatment planning. The execution strategy of the algorithm is detailed in Algorithm 1. The input to the SVM classifier is the feature set of dimension  $n \times m$  which classifies into different lung diseases (where  $n$  and  $m$  are the number of input images and feature count respectively).

Algorithm 1:

**Input:** Training data  $(X_i, Y_i)$  where  $X_i$  represents the feature vectors and  $Y_i$  represents the corresponding class labels.

**Output:** Prediction for a new feature vector  $X$ .

1. Preprocess the input data if necessary (e.g., feature scaling, normalization).
2. Train the SVM model: a) Select a kernel function (e.g., linear, polynomial, radial basis function). b) Define the SVM model with the chosen kernel and appropriate hyperparameters. c) Construct the optimization problem by formulating the SVM objective function. d) Solve the optimization problem to find the optimal separating hyperplane.
3. For a new feature vector  $X$ : a) Apply the same preprocessing steps as in the training phase. b) Calculate the decision function or distance of  $X$  from the separating hyperplane. c) Classify  $X$  based on the sign of the decision function:  
If the decision function is positive, assign  $X$  to one class. If the decision function is negative, assign  $X$  to the other class. If the decision function is zero, assign  $X$  to the class based on a predefined rule (e.g., majority vote).
4. Repeat step 3 for each new feature vector to obtain predictions.

The SVM algorithm aims to find an optimal hyperplane that separates the input data into different classes. The selection of a suitable kernel function and hyperparameters significantly impacts the model's performance and the ability to capture complex relationships in the data. By maximizing the margin between classes, SVM can achieve robust and accurate classification results in various medical imaging applications.

## 3.6 Performance Evaluation

For evaluating the performance of classifiers, Accuracy (Ac), precision (P), re-call, and f1-score are calculated as shown in Equation (5-8), where TP is a true positive value, TN is a true negative value, FP is a false positive value, and FN is a false negative value:

Accuracy represents the overall correctness of a classification model. It calculates the proportion of correctly classified instances (both true positives and true negatives) out of the total number of instances.

$$Accuracy = \frac{TP + TN}{TP + TN + FP + FN} \quad (5)$$

Precision is a measure of how many of the positively classified instances are actually true positives. It calculates the proportion of true positives out of the total number of instances classified as positive.

$$Precision = \frac{TP}{TP + FP} \quad (6)$$

Recall, also known as sensitivity or true positive rate, measures the ability of a model to correctly identify positive instances. It calculates the proportion of true positives out of the total number of actual positive instances.

$$Recall = \frac{TP}{TP + FN} \quad (7)$$

F1-score is a metric that combines both precision and recall into a single value. It calculates the harmonic mean of precision and recall, providing a balanced measure that takes into account both false positives and false negatives. It is commonly used when there is an imbalance between the classes in the dataset.

$$F1 - score = \frac{2 * Precision * Recall}{precision + Recall} \quad (8)$$

## Chapter 4

# Experimental Analysis and Results

### 4.1 Experimental Setup

Python is used to implement the proposed model, taking advantage of various libraries such as Keras, TensorFlow, OpenCV, pandas, scikit-image, NumPy, and others. These libraries provide essential functionalities for image processing, deep learning, data manipulation, and numerical computations. Comparing the performance of the suggested model on a Windows 10 system with a 2.60 GHz Intel Core i7-10750H processor, 16 GB of RAM, and 4 GB of NVIDIA GEFORCE GTX 1650 Ti graphics, it is expected to achieve efficient analysis and training. To ensure accurate evaluation, the NIH chest xray dataset, Lung disease dataset, JSRT dataset are utilized for training and testing purposes. This datasets, sourced from Kaggle, provides a comprehensive collection of chest X-ray images, making it suitable for training models to classify lung diseases accurately.

### 4.2 Datasets

- NIH chest xray dataset

The dataset[21] comprises a collection of 5606 frontal chest radiographs, each annotated with 14 different thoracic pathologies, including Atelectasis, Consolidation, Infiltration, Pneumothorax, Edema, Emphysema, Fibrosis, Effusion, Pneumonia, Pleural thickening, Cardiomegaly, Nodule, Mass, Hernia, and No finding. This dataset provides a diverse range of lung diseases and conditions commonly encountered in medical practice. For the experiment, a total of 4497 images were designated as the training set. This subset is typically used to train machine learning models, enabling them to learn patterns and features associated with different thoracic pathologies. Out of the 1448 images in the dataset, 777 were assigned as the test set. The remaining images were allocated as the validation set. On the validation dataset, the suggested model has 100% accuracy rate. While accuracy is a valuable metric, it is important to consider other evaluation measures to obtain a comprehensive assessment of the model's performance. Metrics such as precision, recall and F1 score can provide deeper insights into the model's ability to correctly identify specific pathologies and differentiate between different classes.

Few samples from the dataset are shown in Figure 4.1.

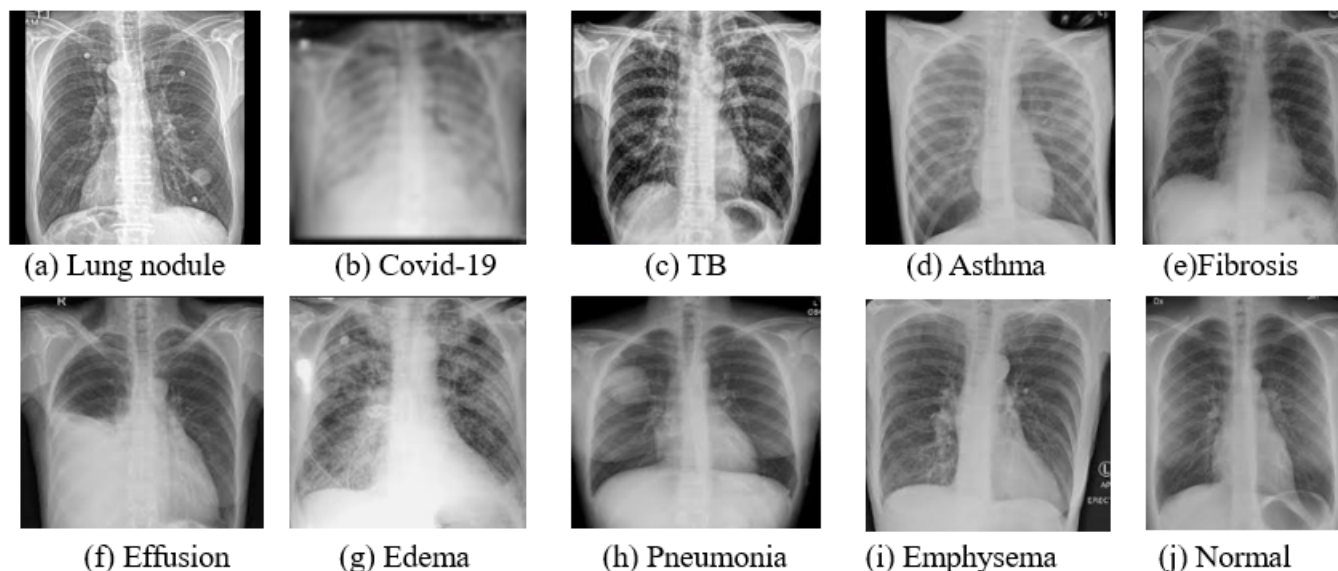


Figure 4.1: Chest xray samples from dataset

Table 4.1 shows the performance matrix and figure 4.2 shows the confusion matrix of the proposed model using NIH dataset.

- Lung disease dataset

The dataset[22] contain Chest X-Rays of Viral Pneumonia, Bacterial Pneumonia, Covid ,Tuberculosis and normal condition. It is a combination of : Covid-19 dataset, Pneumonia dataset, TB chest Xray dataset. The database contains 10,095 CXR images. In order to conduct the experiment, 6054 training images were used, 2016 images were taken as test set and remaining images are considered as validation set. On the validation dataset, the suggested model has 100% accuracy rate. Table 4.2 shows the performance matrix and figure 4.3 shows the confusion matrix using Lung disease dataset.

- JSRT dataset

JSRT database[23] contains 247 digitized CXR images, among which, 154 contain lung nodules and the remaining 93 are normal. In order to conduct the experiment, nodule images were used. The classes are represented by state of nodule such as malignant and benign. On the validation dataset, the suggested model has 96% accuracy rate. Table 4.3 shows the performance matrix and figure 4.4 shows the confusion matrix using JSRT dataset.

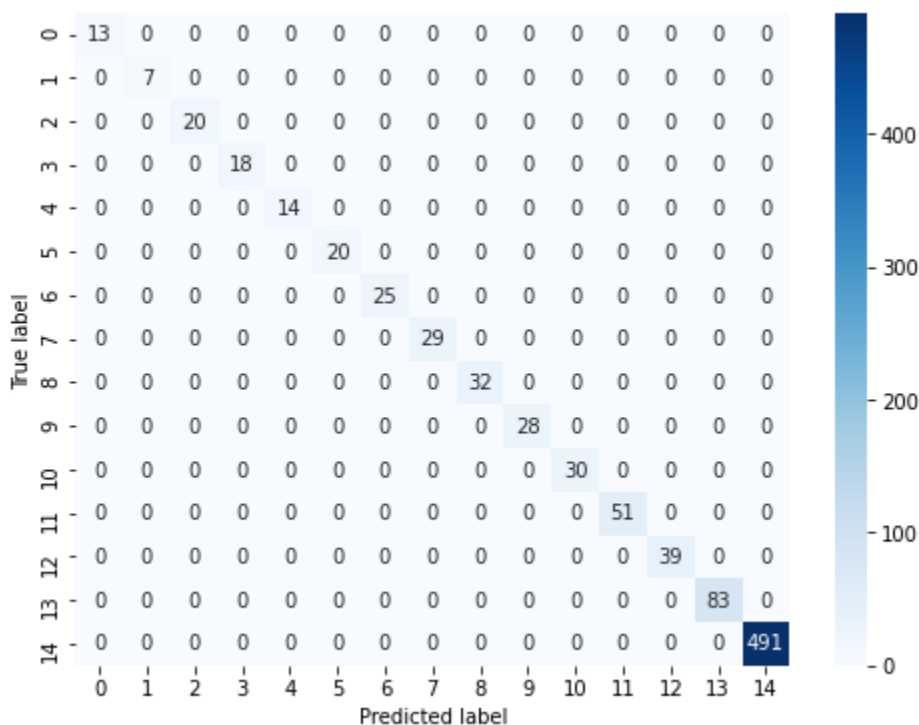


Figure 4.2: Confusion matrix of proposed model using NIH dataset

Table 4.4,4.5,4.6 displays the performance of each dataset with different classifiers in terms of accuracy, precision, recall and f1-score;

### 4.3 Confusion matrix

Confusion matrices are widely used in the field of machine learning and data analysis, particularly in multiclass classification problems. They provide a way to assess the performance of a multiclass classification model by comparing the expected (true) class labels with the predicted (observed) class labels. In a multiclass classification confusion matrix, the matrix is square, with each row and column representing a different class in the classification problem. The entries in the matrix represent the counts or frequencies of different outcomes based on the predictions made by the model. The main components of a multiclass classification confusion matrix are:

Table 4.1: Performance metrics of proposed model using NIH dataset

	<b>Precision</b>	<b>recall</b>	<b>f1-score</b>
Hernia	100%	100%	100%
Pneumonia	100%	100%	100%
Fibrosis	100%	100%	100%
Edema	100%	100%	100%
Emphysema	100%	100%	100%
Cardiomegaly	100%	100%	100%
Pleural Thickening	100%	100%	100%
Consolidation	100%	100%	100%
Pneumothorax	100%	100%	100%
Mass	100%	100%	100%
Nodule	100%	100%	100%
Atelectasis	100%	100%	100%
Effusion	100%	100%	100%
Infiltration	100%	100%	100%
No Finding	100%	100%	100%

Table 4.2: Performance metrics of proposed model using Lung disease dataset

	<b>Precision</b>	<b>recall</b>	<b>f1-score</b>
Bacterial Pneumonia	100%	100%	100%
Corona Virus Disease	100%	100%	100%
Normal	100%	100%	100%
Tuberculosis	100%	100%	100%
Viral Pneumonia	100%	100%	100%

- True Positives (TP): It represents the number of instances that are correctly classified for each class. These are the cases where the model made the correct prediction of the corresponding class.
- True Negatives (TN): It represents the number of instances that are correctly classified as negative for each class other than the one under consideration. In a multiclass problem, this value is not applicable for the specific class being evaluated and is usually not considered.
- False Positives (FP): It represents the number of instances that are incorrectly classified as positive for each class. These are the cases where the model made a false prediction of the corresponding class.
- False Negatives (FN): It represents the number of instances that are incorrectly classified as negative for each class. These are the cases where the model failed to recognize the corresponding class.

From the confusion matrix, various evaluation metrics can be calculated for each class,

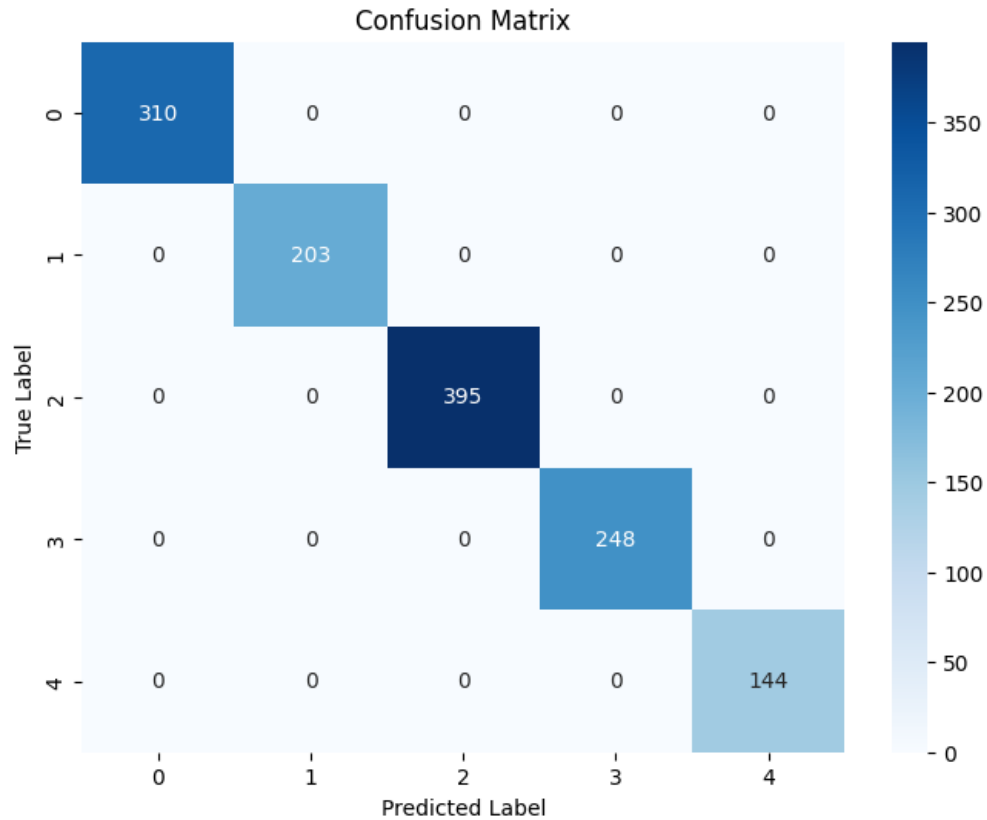


Figure 4.3: Confusion matrix using Lung disease dataset

such as accuracy, precision, recall (sensitivity), specificity, and F1-score. These metrics provide a more detailed understanding of the model’s performance on individual classes and can guide further improvements. Analyzing the confusion matrix for multiclass classification problems helps in identifying patterns of misclassifications, understanding the strengths and weaknesses of the model for different classes.

#### 4.4 ROC - AUC

The Receiver Operating Characteristic Area Under the Curve (ROC-AUC) is a performance metric commonly used in classification problems. It measures the ability of a classification model to distinguish between positive and negative classes by plotting the true positive rate (TPR) against the false positive rate (FPR) at various classification thresholds. The ROC curve is created by varying the threshold that separates the positive and negative predictions, and for each threshold, calculating the corresponding TPR and FPR values. The area under the ROC curve, known as the ROC-AUC, provides a single value that represents the overall performance of the classifier. The higher the ROC-AUC score, the better the classifier’s ability to correctly classify positive

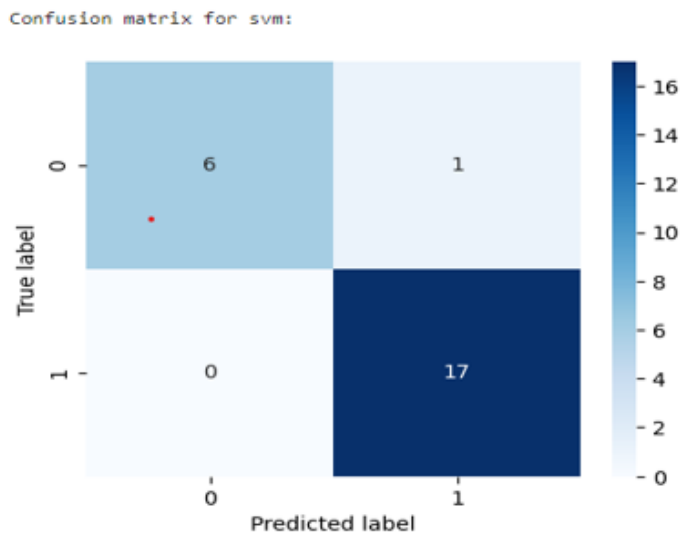


Figure 4.4: Confusion matrix using JSRT dataset.

Table 4.3: Performance metrics of proposed model using JSRT dataset

	<b>Precision</b>	<b>recall</b>	<b>f1-score</b>
Benign	100%	86%	92%
Malignant	94%	100%	97%

instances and distinguish them from negative instances.

An ROC-AUC score of 1 indicates a perfect classifier, while a score of 0.5 suggests a classifier that performs no better than random guessing. ROC-AUC is particularly useful in situations where class imbalance exists or when the costs of false positives and false negatives are different. It's important to note that ROC-AUC is primarily applicable to binary classification problems. For multi-class classification, variations of the ROC-AUC metric, such as the one-vs-all approach or averaging the scores across classes, can be used to assess the classifier's performance. In addition to this, figure 4.5 shows the ROC-AUC curve of proposed Wavelet CNN model. From the figure, it can be observed that we obtain an ideal ROC AUC curve as a straight line. The ROC AUC score also tells that the model is able to perfectly separate the chest X ray images.

## 4.5 Comparison with Existing Works

Table 4.7 shows the comparison of proposed model with existing works. Among the existing works, Vieira et al. (2021) utilized a CNN model and achieved an accuracy of 99.8% using the NIH, Pneumonia, and Covid-19 datasets with four classes. Ismael et al. (2022) employed a CNN combined with SVM and achieved an accuracy of 94.7% on

Table 4.4: Comparison between different classifiers using NIH dataset

<b>Classifier</b>	<b>Accuracy</b>	<b>Precision</b>	<b>recall</b>	<b>f1-score</b>
SVM	100%	100%	100%	100%
Decision tree	96%	90%	84%	82%
Random forest	57%	51%	58%	47%
Naive Bayes	96%	90%	88%	82%
KNN	62%	55%	51%	44%

Table 4.5: Comparison between different classifiers using Lung disease dataset

<b>Classifier</b>	<b>Accuracy</b>	<b>Precision</b>	<b>recall</b>	<b>f1-score</b>
SVM	100%	100%	100%	100%
Decision tree	98%	90%	87%	88%
Random forest	68%	67%	68%	67%
Naive Bayes	93%	94%	93%	92%
KNN	79%	70%	70%	69%

the Covid-19 dataset with two classes. Bharati et al. (2020) utilized a CNN on the NIH dataset with two classes and achieved an accuracy of 69.5%. Li et al. (2020) employed a CNN on the JSRT dataset with two classes and achieved an accuracy of 98%. Li et al. (2018) used an E-CNN on the JSRT dataset with two classes and achieved an accuracy of 84%.

In comparison to these existing works, the proposed method, which combines wavelet-based CNNs with an SVM classifier, achieves outstanding results. It demonstrates 100% accuracy on the NIH dataset with 15 classes, 100% accuracy on the LUNG DISEASE dataset with five classes, and 96% accuracy on the JSRT dataset with two classes. These results highlight the superiority of the proposed method in accurately classifying various lung diseases compared to the existing approaches.

The table summarizes the performance of different methods, showcasing the significant improvements achieved by the proposed method. The use of wavelet-based CNNs in combination with an SVM classifier proves to be highly effective in achieving remarkable accuracy rates across multiple datasets and diverse classes. These findings demonstrate the potential of the proposed method for accurate and efficient lung disease identification, contributing to the advancement of medical imaging and diagnosis.

# WAVELET BASED CNN FOR DIAGNOSIS OF LUNG DISEASES USING CHEST X-RAYS

Table 4.6: Comparison between different classifiers using JSRT dataset

Classifier	Accuracy	Precision	recall	f1-score
SVM	96%	97%	93%	95%
Decision tree	96%	97%	95%	96%
Random forest	70%	67%	68%	67%
Naive Bayes	75%	86%	62%	62%
KNN	58%	55%	51%	44%

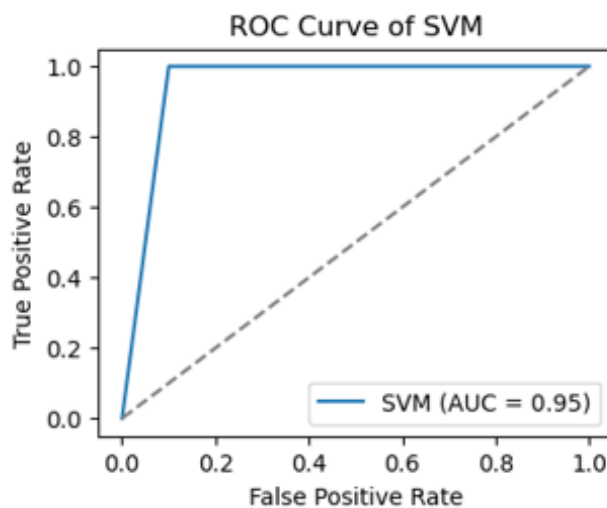


Figure 4.5: ROC-AUC curve of proposed model using JSRT dataset

Table 4.7: Comparison with Existing Works

Author	Methodology	dataset	Classes	Performance
Vieira et al. [8]	CNN	NIH, Pneumonia, Covid-19 dataset	4 classes	Acc - 99.8%
Ismael et al. [9]	CNN + SVM	Covid-19 dataset	2 classes	Acc - 94.7%
Bharati et al. [12]	CNN	NIH dataset	2 classes	Acc - 69.5%
Li et al. [13]	CNN	JSRT dataset	2 classes	Acc - 98%
Li et al. [17]	E-CNN	JSRT dataset	2 classes	Acc - 84%
Proposed method	Wavelet CNN + SVM	NIH dataset	15 classes	Acc - 100%
Proposed method	Wavelet CNN+ SVM	LUNG DISEASE dataset	5 classes	Acc - 100%
Proposed method	Wavelet CNN + SVM	JSRT dataset	2 classes	Acc - 96%

## Chapter 5

# Conclusion

This study introduces a novel approach for classifying lung diseases based on chest X-ray images. The proposed framework combines wavelet-based Convolutional Neural Networks (CNNs) with a Support Vector Machine (SVM) classifier, resulting in a highly accurate method for detecting and distinguishing different types of lung diseases. One key aspect of the proposed approach is the use of wavelets, which enable the decomposition of the X-ray images into multiple spatial resolutions. By extracting features from the affected areas efficiently, this approach addresses a limitation of traditional CNN architectures that process images in a single resolution. By incorporating information from different resolutions, potential features that might be missed by a single-resolution approach can be captured effectively.

To evaluate the effectiveness of the proposed approach, extensive testing was conducted on three publicly available datasets: NIH Chest X-ray, LUNG DISEASE, and JSRT. The results demonstrate impressive performance, with an average accuracy of 100% on the NIH dataset, 100% accuracy on the LUNG DISEASE dataset, and 96% accuracy on the JSRT dataset. These results outperform existing works in the field, highlighting the superiority of the proposed framework. Another notable aspect of the proposed approach is its versatility in identifying various lung conditions, including nodules, COVID-19, and other ailments. This broad applicability enhances its value in providing prompt and accurate diagnoses of a wide range of lung diseases.

The study emphasizes the potential of wavelet-based CNNs in the analysis of chest X-ray images for lung disease classification. The achieved high accuracy and the capability to identify diverse conditions make this approach a promising and versatile tool in the field of medical imaging and diagnosis. The findings of this study contribute to advancements in the field of lung disease detection and have the potential to improve patient outcomes through more accurate and efficient diagnoses. In the future, the proposed approach for real-time classification of lung diseases based on chest X-ray images holds significant potential for transforming medical imaging and diagnosis. Real-time lung disease classification will enable healthcare professionals to make immediate and informed decisions, provide remote healthcare services, and empower patients with accessible and timely diagnoses, ultimately improving patient outcomes.

# References

- [1] Coudray, N., Ocampo, P.S., Sakellaropoulos, T., Narula, N., Snuderl, M., Fenyö, D., Moreira, A.L., Razavian, N. and Tsirigos, A., 2018. Classification and mutation prediction from non-small cell lung cancer histopathology images using deep learning. *Nature medicine*, 24(10), pp.1559-1567.
- [2] Bharati, S., Podder, P., Mondal, R., Mahmood, A. and Raihan-Al-Masud, M., 2020. Comparative performance analysis of different classification algorithm for the purpose of prediction of lung cancer. In *Intelligent Systems Design and Applications: 18th International Conference on Intelligent Systems Design and Applications (ISDA 2018) held in Vellore, India, December 6-8, 2018, Volume 2* (pp. 447-457). Springer International Publishing.
- [3] Mondal, M.R.H., Bharati, S., Podder, P. and Podder, P., 2020. Data analytics for novel coronavirus disease. *informatics in medicine unlocked*, 20, p.100374.
- [4] Kuan, K., Ravaut, M., Manek, G., Chen, H., Lin, J., Nazir, B., Chen, C., Howe, T.C., Zeng, Z. and Chandrasekhar, V., 2017. Deep learning for lung cancer detection: tackling the kaggle data science bowl 2017 challenge. *arXiv preprint arXiv:1705.09435*.
- [5] Sun, W., Zheng, B. and Qian, W., 2017. Automatic feature learning using multi-channel ROI based on deep structured algorithms for computerized lung cancer diagnosis. *Computers in biology and medicine*, 89, pp.530-539.
- [6] Song, Q., Zhao, L., Luo, X. and Dou, X., 2017. Using deep learning for classification of lung nodules on computed tomography images. *Journal of healthcare engineering*, 2017.
- [7] Sun, W., Zheng, B. and Qian, W., 2016, March. Computer aided lung cancer diagnosis with deep learning algorithms. In *Medical imaging 2016: computer-aided diagnosis* (Vol. 9785, pp. 241-248). SPIE.
- [8] Vieira, P., Sousa, O., Magalhães, D., Rabêlo, R. and Silva, R., 2021. Detecting pulmonary diseases using deep features in X-ray images. *Pattern Recognition*, 119, p.108081.
- [9] Ismael, A.M. and Şengür, A., 2021. Deep learning approaches for COVID-19 detection based on chest X-ray images. *Expert Systems with Applications*, 164, p.114054.
- [10] Shah, P.M., Ullah, F., Shah, D., Gani, A., Maple, C., Wang, Y., Abrar, M. and Islam, S.U., 2021. Deep GRU-CNN model for COVID-19 detection from chest X-rays data. *Ieee Access*, 10, pp.35094-35105.

- [11] Mehrrotraa, R., Ansari, M.A., Agrawal, R., Tripathi, P., Heyat, M.B.B., Al-Sarem, M., Muaad, A.Y.M., Nagmeldin, W.A.E., Abdelmaboud, A. and Saeed, F., 2022. Ensembling of efficient deep convolutional networks and machine learning algorithms for resource effective detection of tuberculosis using thoracic (chest) radiography. *IEEE Access*, 10, pp.85442-85458.
- [12] Bharati, S., Podder, P. and Mondal, M.R.H., 2020. Hybrid deep learning for detecting lung diseases from X-ray images. *Informatics in Medicine Unlocked*, 20, p.100391.
- [13] Li, X., Shen, L., Xie, X., Huang, S., Xie, Z., Hong, X. and Yu, J., 2020. Multi-resolution convolutional networks for chest X-ray radiograph based lung nodule detection. *Artificial intelligence in medicine*, 103, p.101744.
- [14] Makris, A., Kontopoulos, I. and Tserpes, K., 2020, September. COVID-19 detection from chest X-Ray images using Deep Learning and Convolutional Neural Networks. In *11th hellenic conference on artificial intelligence* (pp. 60-66).
- [15] de Moura, J., Novo, J. and Ortega, M., 2022. Fully automatic deep convolutional approaches for the analysis of COVID-19 using chest X-ray images. *Applied Soft Computing*, 115, p.108190.
- [16] Ayan, E., Karabulut, B. and Ünver, H.M., 2022. Diagnosis of pediatric pneumonia with ensemble of deep convolutional neural networks in chest x-ray images. *Arabian Journal for Science and Engineering*, pp.1-17.
- [17] Li, C., Zhu, G., Wu, X. and Wang, Y., 2018. False-positive reduction on lung nodules detection in chest radiographs by ensemble of convolutional neural networks. *IEEE Access*, 6, pp.16060-16067.
- [18] Hemdan, E.E.D., Shouman, M.A. and Karar, M.E., 2020. Covidx-net: A framework of deep learning classifiers to diagnose covid-19 in x-ray images. *arXiv preprint arXiv:2003.11055*.
- [19] Kakde, A., Sharma, D. and Arora, N., 2020. Optimal Classification of COVID-19: A Transfer Learning Approach. *Int. J. Comput. Appl*, 176(20), pp.25-31.
- [20] Yasar, H. and Ceylan, M., 2021. A new deep learning pipeline to detect Covid-19 on chest X-ray images using local binary pattern, dual tree complex wavelet transform and convolutional neural networks. *Applied Intelligence*, 51, pp.2740-2763.
- [21] NATIONAL INSTITUTES OF HEALTH CHEST X-RAY DATASET. (2017,July). NIH chest X-ray dataset, Version 1.Retrieved December,2022 from <https://www.kaggle.com/datasets/nih-chest-xrays/sample>.
- [22] OMKAR MANOHAR DALVI.(2022,July). LungsDiseaseDataset, Version 1.Retrieved December,2022 from <https://www.kaggle.com/datasets/omkarmanohardalvi/lungs-disease-dataset-4-types>.
- [23] RADDAR. (2000,August). Nodules in Chest X-rays(JSRT) dataset, Version 1.Retrieved December,2022 from <https://www.kaggle.com/datasets/raddar/nodules-in-chest-xrays-jsrt>.